Original Article

YISHENJUANBI PILL-CONTAINING SERUM ATTENUATES OSTEOCLASTOGENESIS IN OVARIECTOMIZED RATS WITH COLLAGEN-INDUCED ARTHRITIS BY ENHANCING EPHRINB2 SIGNALLING

Y.Y. Wang[1,§], H.H. Xu[2,§], J.F. Cao[1], H. Liu[1], J.H. Pan[1], Y. Li[1], S.J. Wang[1], L. Tang[3], H.R. Ju[4], Y.S. Shi[5], D.P. Fan[1,*] and H.Y. Zhao[1,*]

[1]Experimental Research Center, China Academy of Chinese Medical Sciences, 100010 Beijing, China
[2]Department of Joints and Soft Tissue Injury, Shenzhen Traditional Chinese Medicine Hospital, The Fourth Clinical Medical College of Guangzhou University of Chinese Medicine, 518000 Shenzhen, Guangdong, China
[3]Department of Cardiovascular Sciences and Center for Metabolic Disease Research, Lewis Katz School of Medicine, USA Temple University, Philadelphia, PA 19140, USA
[4]Health Science Center, Peking University, 100091 Beijing, China
[5]China College of Exercise and Health, Jilin Sport University, 130022 Changchun, Jilin, China
[§]These authors contributed equally.

Abstract

Background: Rheumatoid arthritis (RA) disproportionately affects postmenopausal women and manifests as accelerated cartilage and bone erosion driven by hyperactive osteoclasts (OCs). Oestrogen deficiency exacerbates OC activity, while the Eph receptor interacting protein B2 (EphrinB2)/Eph receptor B4 (EphB4) signalling pathway acts as a critical negative regulator of OC differentiation by suppressing the cellular oncogene c-Fos (c-Fos)/nuclear factor of activated T cells cytoplasmic 1 (NFATc1) transcription cascade. The traditional Chinese medicine (TCM) Yishenjuanbi pill (YSJB) enhances EphrinB2-mediated bone protection and demonstrates superior therapeutic efficacy in an ovariectomized collagen-induced arthritis (OVX + CIA) rat model compared with its effects in CIA rats, although its effects on osteoclasts (OCs) remain incompletely characterized. **Methods**: Bone marrow-derived macrophages (BMMs) and splenic monocytes were employed to elucidate the EphrinB2-dependent mechanisms through which YSJB inhibits OC differentiation. Rat serum from the Control, OVX, CIA, OVX + CIA, OVX + CIA + oestradiol valerate (EV), and OVX + CIA + YSJB groups was prepared and added during osteoclast induction. Quantitative reverse transcription PCR (RT-qPCR), tartrate-resistant acid phosphatase (TRAP) staining, and bone resorption assays were performed on both cell types. **Results**: YSJB reversed the ovariectomy + CIA-induced upregulation of the osteoclastogenic factors c-Fos, transcription factor c-Jun (c-Jun), Nfatc1, and receptor activator of nuclear factor-κb (Rank) while restoring encoding EphrinB2 (Efnb2) expression (n = 3). Crucially, *Efnb2* knockdown abolished the protective effects of YSJB, restoring pathological OC activity and increasing gene expression levels (n = 3). **Conclusions**: Our findings suggest that by upregulating EphrinB2, YSJB serum inhibits osteoclastogenesis in both BMMs and splenic monocytes.

Keywords: Collagen-induced arthritis, osteoclasts, Yishenjuanbi pill, EphrinB2 signalling pathway.

***Address for correspondence**: H.Y. Zhao, Experimental Research Center, China Academy of Chinese Medical Sciences, 100010 Beijing, China. Email: zhaohongyan1997@163.com; D.P. Fan, Experimental Research Center, China Academy of Chinese Medical Sciences, 100010 Beijing, China. Email: zgzyfdp@126.com.

Introduction

Rheumatoid arthritis (RA) is an autoimmune disease characterized by chronic synovitis and pannus formation, with a pathological progression that induces progressive erosion of adjacent cartilage and bone tissue, ultimately leading to destruction of the joint structure [1]. The incidence of RA has a marked sex disparity, with a prevalence approximately threefold greater in females than in males, and a particularly sharp increase among postmenopausal women [2]. Notably, oestrogen replacement therapy or pregnancy is often correlated with significant symptomatic remission in female patients with RA [3,4]. Studies have demonstrated that ovariectomized (OVX) exacerbates joint inflammation, bone loss, and skeletal muscle atrophy in collagen-induced arthritis (CIA) model mice/rats, whereas oestrogen supplementation effectively attenuates bone loss and joint destruction [5,6].

Osteoclasts (OCs) are the only bone-resorbing cells and play a pivotal role in the destruction of cartilage and bone in the context of RA [7–10]. OC precursors from RA patients are more susceptible to differentiation into functionally active OCs under inflammatory conditions, leading to significant accumulation of both OCs and their precursors at RA lesion sites [11]. *In vitro* differentiation models are essential tools for exploring the regulation of OC differentiation. Specifically, bone marrow-derived mononuclear macrophages—a classic model of OC precursors—can efficiently differentiate into mature OCs when stimulated by key cytokines such as macrophage colony-stimulating factor (M-CSF) and receptor activator of nuclear factor-κB ligand (RANKL) [12–14]. These precursors are present in the bone marrow, peripheral blood, and spleen. Bone marrow-derived macrophages (BMMs), as classical OC precursors, represent a primary model for studying the biological characteristics and differentiation regulation of OCs [15,16]. BMMs play a critical role in inflammatory responses, cartilage repair, and subchondral bone remodeling [17]. Notably, monocytes from the peripheral blood or spleen also possess osteoclastogenic potential under certain conditions [18,19], offering a valuable model for investigating immune-related OC differentiation. However, research in this domain remains relatively limited. Previous studies have demonstrated that induced inflammation markedly increases the proportion of cells with osteogenic potential in the bone marrow and spleen [20,21]. These findings suggest that inflammatory conditions may amplify OC formation, thereby accelerating pathological bone destruction in patients with RA.

Eph receptor interacting protein B2 (EphrinB2), a membrane-bound protein, facilitates the transmission of crucial intercellular signals via interactions with Eph receptors [22–24]. The bidirectional EphrinB2/Eph receptor B4 (EphB4) signalling pathway is critical for bone homeostasis regulation, coupling the inhibition of OC differentiation to the promotion of bone formation [25,26]. Importantly, the critical osteoclastogenic transcription cascade mediated by cellular oncogene c-Fos (c-Fos)/nuclear factor of activated T cells cytoplasmic 1 (NFATc1) is controlled by an EphrinB2-mediated negative feedback mechanism. During OC differentiation, EphrinB2 expression is dependent on the RANKL-induced c-Fos/NFATc1 cascade. Furthermore, EphrinB2 subsequently exerts reciprocal feedback inhibition on the transcription of both c-Fos and its downstream target Nfatc1 [27]. Our prior research revealed that EphrinB2 and its receptor EphB4 are crucial for the regulation of bone metabolism in an ovariectomized collagen-induced arthritis (OVX + CIA) rat model. Under RA-like pathology, OC numbers in both synovial and bone marrow tissues significantly increase. Critically, Yishenjuanbi pill (YSJB) has been shown to upregulate EphrinB2, downregulate OC differentiation transcription factors, and consequently inhibit OC differentiation while ameliorating bone destruction (as evidenced by three-dimensional (3D) micro-computed tomography (CT) reconstructions) in OVX + CIA rat models.

In traditional Chinese medicine (TCM) theory, RA is categorized as “Bi Zheng” (Arthralgia Syndrome), with “Kidney Deficiency Syndrome” being the most common pattern. Therefore, “tonifying the kidney” is a crucial therapeutic principle for RA treatment. YSJB, a TCM compound formulated by renowned physician Professor Zhu Liangchun, is precisely based on the concept of “treating arthralgia by first tonifying the kidney.” Since its approval in 1987, YSJB has demonstrated significant efficacy and safety in RA clinical applications [28]. The formula incorporates multiple typical kidney-tonifying herbs, such as Herba Cistanchis (Cistanche), Herba Epimedii (Epimedium), and Radix Rehmanniae Preparata (processed Rehmannia root). These herbs, according to TCM theory, nourish kidney essence and strengthen bones and tendons, directly targeting the root pathogenesis of “kidney deficiency.” Postmenopausal status exhibits parallels with TCM kidney deficiency syndrome in key pathological features, including accelerated bone loss and a pro-inflammatory bone marrow microenvironment [29,30]. Our prior research established a link between the TCM “Kidney Deficiency” pattern and the modern medical state of “sex hormone deficiency.” We found that low sex hormone status significantly exacerbates arthritis indices and bone destruction in CIA rats. YSJB effectively reduces pro-inflammatory cytokine interleukin (IL)-6 levels while elevating anti-inflammatory cytokine IL-10 levels, thereby correcting immune dysregulation under “Kidney Deficiency” conditions. In exploring the pharmacological mechanisms of YSJB, our high performance liquid chromatography (HPLC) analysis identified primary active components in YSJB-containing serum-monotropein and paeonol. Subsequent *in vitro* experiments demonstrated that YSJB-containing serum targets the Janus kinase 2 (JAK2)/signal transducer and activator of transcrip-

Table 1. Primer sequences used in this study.

Gene	Sense primer sequence (5′–3′)	Antisense primer sequence (5′–3′)
GAPDH	GGTTGTCTCCTGCGACTTCA	TGGTCCAGGGTTTCTTACTCC
c-Fos	CGTCTTCCTTTGTCTTCACCTACCC	TTGCTGCTGCTGCCCTTTCG
c-Jun	CAGCCGCCGCACCACTTG	TGATCCGCTCCTGAGACTCCATG
Nfatc1	CATCCTTGCCTGCCCTTGACTG	TGAGCCCTGTGGTGAGACTTGG
Rank	FATGGAAGGCTCATGGTTGGATGTG	GAGTGACTTTATGGGAACCCGATGG
Efnb2	TAGTCTTCCTCATCGCTGTG	ATGATGGATGCCTCACTCAG

tion 3 (STAT3) signaling pathway, exerting dual regulatory effects: directly inhibiting osteoclast differentiation and bone resorption by downregulating the RANK/NFATc1/c-fos pathway, and indirectly suppressing osteoclasts by enhancing Tregs' IL-10 secretion to improve the immunosuppressive microenvironment [31]. Our *in vivo* study confirmed that OVX exacerbates arthritis severity in CIA rats, while YSJB treatment significantly reduces arthritis index (AI) scores and improves joint histopathology, including reduced synovial hyperplasia and inflammatory cell infiltration. Micro-CT analysis of bone microstructure revealed that YSJB improves bone parameters in OVX + CIA rats, evidenced by increased bone volume (BV) and decreased bone surface/bone volume ratio (BS/BV). Immunohistochemical analysis showed that YSJB downregulates the key osteoclast transcription factor NFATc1 in synovial tissue, and it upregulates EphrinB2 and downregulates NFATc1 expression in bone marrow tissue. Building upon this foundation, the present study specifically aims to elucidate the EphrinB2-dependent mechanisms by which YSJB inhibits OC differentiation and function. To achieve this, we employed serum containing YSJB metabolites prepared from OVX + CIA model rats, combined with osteoclastogenesis induction from spleen-derived monocytes and bone marrow-derived mononuclear macrophages *in vitro*. This investigation specifically addresses EphrinB2 signaling-mediated regulation of OC differentiation from these dual cellular sources, seeking to comprehensively delineate YSJB's mechanism of action in modulating OC differentiation and function.

Materials and Methods

Animals

Thirty-five female specific pathogen free (SPF) Sprague-Dawley rats (7–8 weeks old, 180–270 g) were obtained from Peking University Health Science Center (Licence No. SCXK 2016-0010). Thirty female SPF C57BL/6 mice (7–8 weeks old, 18–22 g) were obtained from Beijing Vital River Laboratory Animal Technology (Licence No. SCXK 2019-0009). All the animals were housed under SPF conditions at the Institute of Basic Theory of Traditional Chinese Medicine Experimental Animal Center (Facility Licence No. SYXK 2016-0021).

Drugs

YSJB was provided by Jiangsu Chiatai Qingjiang Pharmaceutical (Huai'an, China, Z10890004). Oestradiol valerate (EV) was obtained from Bayer Delpharm Lille (Lys-lez-Lannoy, France, J20171038).

Ovariectomy and Induction of Collagen-Induced Arthritis

Thirty-five female Sprague-Dawley rats were used in this study. The animals were weight-matched and assigned to the following groups: Control (n = 5), CIA (n = 7), and OVX (n = 23). The rats in the OVX group underwent bilateral ovariectomy under anaesthesia with sodium pentobarbital (Merck, Kenilworth, NJ, USA, 45 mg/kg, P3761) via a dorsolateral incision; the incisions were sutured post-resection.

At 12 weeks after surgery, 5 rats were randomly assigned to the OVX-only group. CIA was then induced in the remaining OVX rats (n = 18) and CIA rats (n = 7). Type II collagen emulsified (Chondrex, Woodinville, WA, USA; 20022) in an equal volume of incomplete Freund's adjuvant (IFA) (Chondrex, Woodinville, WA, USA; 7002) was prepared by dropwise mixing. Each rat received a 0.2 mL subcutaneous emulsion injection at the tail base on day 0. A booster immunization (0.1 mL/rat) was administered in an identical manner on day 7.

Collection of Drug-Containing Serum

Six drug-containing serum groups were established: Control, OVX, CIA, OVX + CIA, OVX + CIA + EV, and OVX + CIA + YSJB. The Control, OVX, and CIA groups were treated as described in "Ovariectomy and Induction of Collagen-Induced Arthritis". Fourteen days after primary immunization, nonarthritic rats were excluded (as per the evaluation protocol established in our prior study, rats demonstrating an arthritic index of 0 were designated for exclusion; however, no such exclusion occurred during the experimental process in this study). The remaining ovariectomized CIA rats were randomized into three groups on the basis of the degree of joint swelling: OVX + CIA, OVX + CIA + EV, and OVX + CIA + YSJB.

The rats in the Control, OVX, CIA, and OVX + CIA groups were orally administered purified water. Rats in the OVX + CIA + YSJB group received a 0.3 g/mL YSJB aqueous solution, while those in the OVX + CIA + EV group were given a 0.0184 mg/mL EV aqueous solution. All the

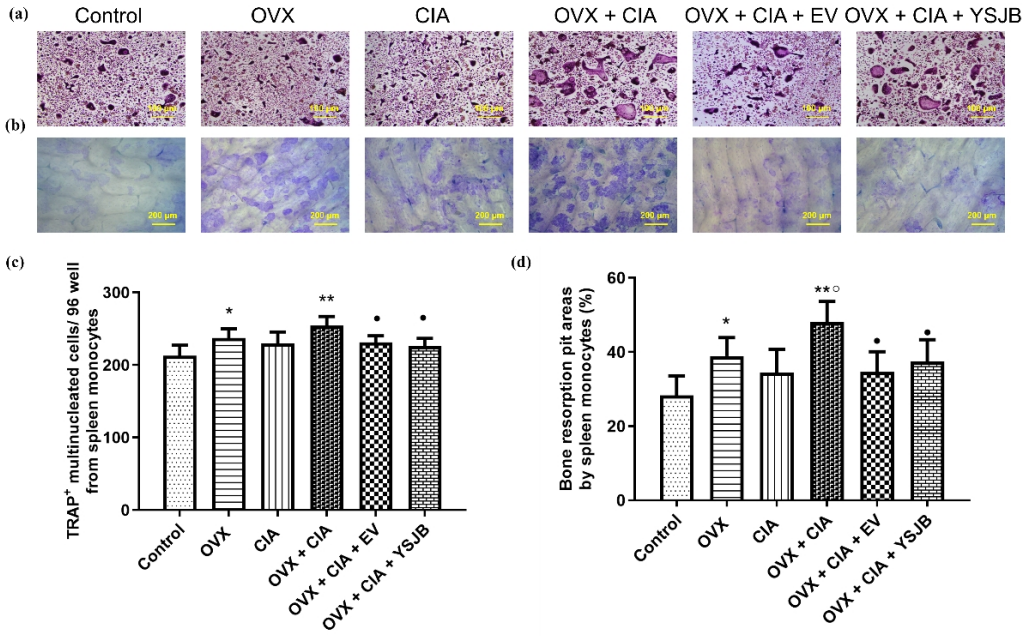

Fig. 1. YSJB inhibits spleen cell differentiation into OCs (TRAP staining) and bone resorption activity (toluidine blue staining). (**a**) OC differentiation in the Control, OVX, CIA, OVX + CIA, OVX + CIA + EV, and OVX + CIA + YSJB groups. The scale bar represents 100 μm. (**b**) Bone resorption activity in the Control, OVX, CIA, OVX + CIA, OVX + CIA + EV, and OVX + CIA + YSJB groups. The scale bar represents 200 μm. (**c**) Quantitative changes in the number of spleen-derived OCs. (**d**) Quantitative changes in the bone erosion area caused by spleen-derived OCs. Statistical comparisons: $^{*}p < 0.05$, $^{**}p < 0.01$ vs. the Control group; $^{\circ}p < 0.05$, vs. the CIA group; $^{\bullet}p < 0.05$, vs. the OVX + CIA group.

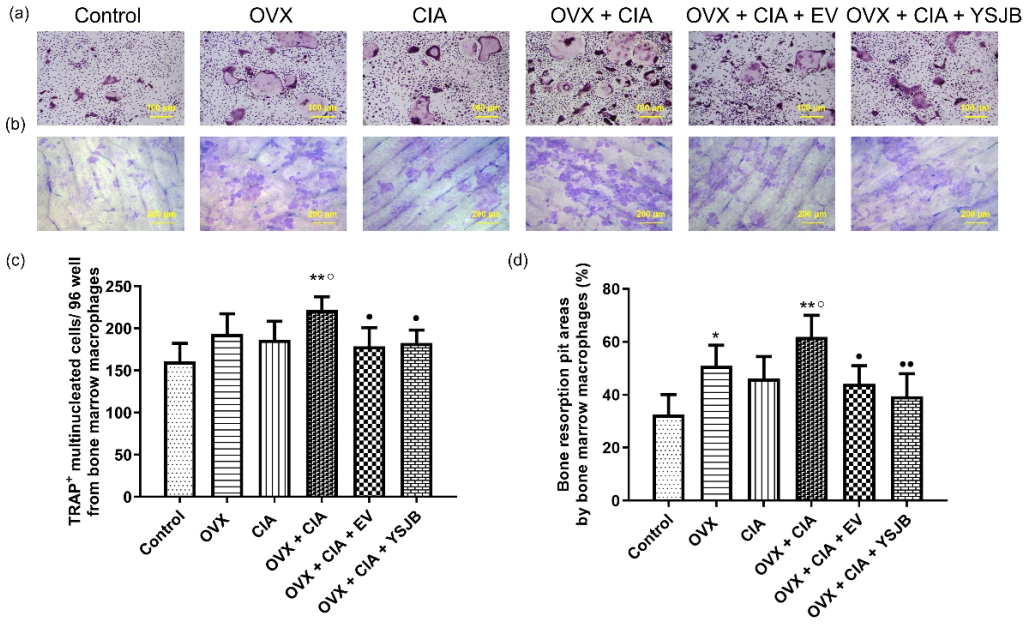

Fig. 2. YSJB inhibits bone marrow cell differentiation into OCs (TRAP staining) and bone resorption activity (toluidine blue staining). (**a**) OC differentiation in the Control, OVX, CIA, OVX + CIA, OVX + CIA + EV, and OVX + CIA + YSJB groups. The scale bar represents 100 μm. (**b**) Bone resorption activity in the Control, OVX, CIA, OVX + CIA, OVX + CIA + EV, and OVX + CIA + YSJB groups. The scale bar represents 200 μm. (**c**) Quantitative changes in the number of bone marrow-derived OCs. (**d**) Quantitative changes in the bone erosion area caused by bone marrow-derived OCs. Statistical comparisons: $^{*}p < 0.05$, $^{**}p < 0.01$ vs. the Control group; $^{\circ}p < 0.05$, vs. the CIA group; $^{\bullet}p < 0.05$, $^{\bullet\bullet}p < 0.01$ vs. the OVX + CIA group.

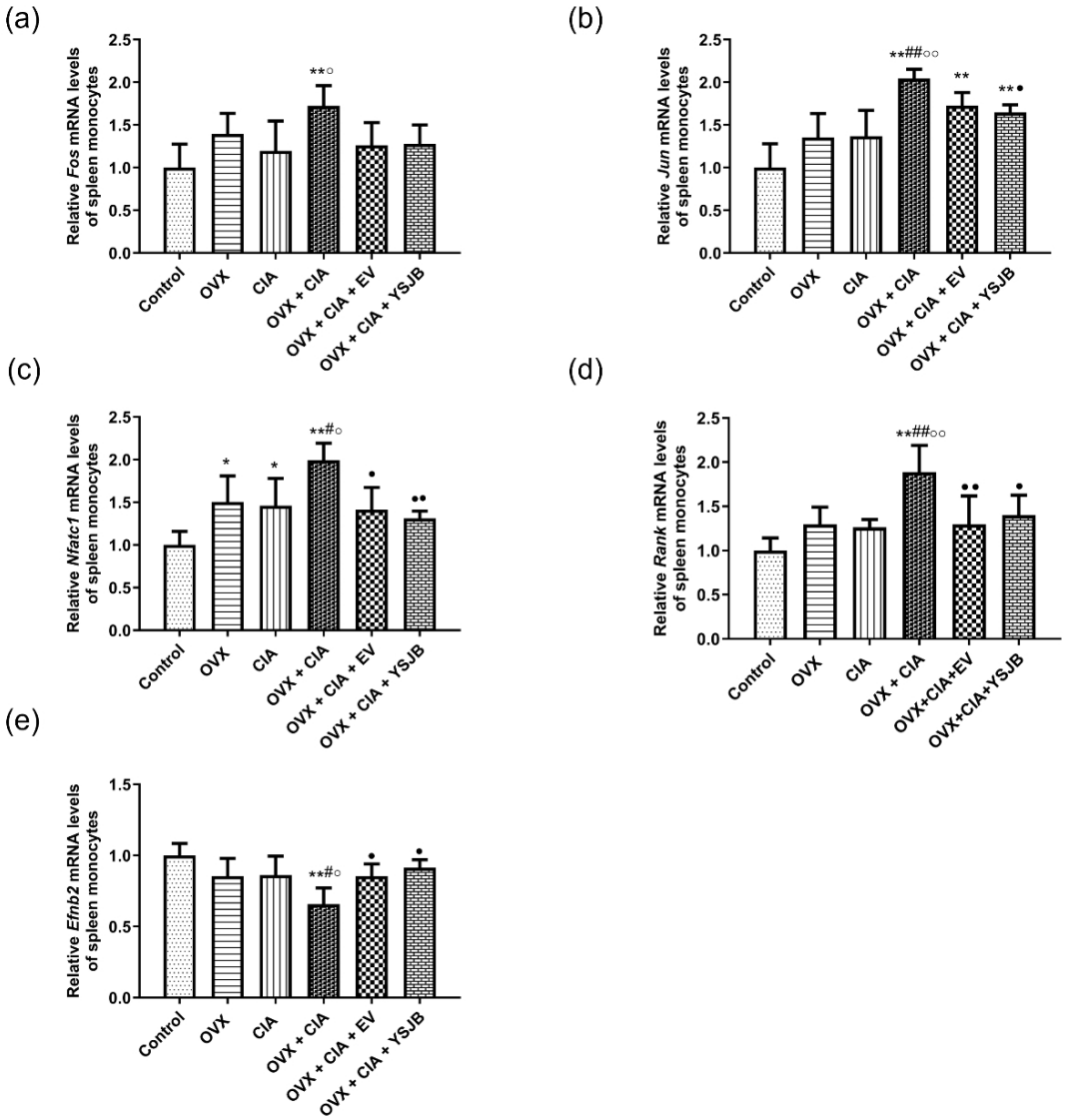

Fig. 3. YSJB upregulates *Efnb2* mRNA expression and inhibits osteoclast-related transcription factor expression in spleen-derived osteoclasts. (**a**) *c-Fos* mRNA expression, (**b**) *c-Jun* mRNA expression, (**c**) *Nfatc1* mRNA expression, (**d**) *Rank* mRNA expression, and (**e**) *Efnb2* mRNA expression. Statistical comparisons: $^{*}p < 0.05$, $^{**}p < 0.01$ vs. the Control group; $^{\#}p < 0.05$, $^{\#\#}p < 0.01$ vs. the OVX group; $^{\circ}p < 0.05$, $^{\circ\circ}p < 0.01$ vs. the CIA group; $^{\bullet}p < 0.05$, $^{\bullet\bullet}p < 0.01$ vs. the OVX + CIA group.

treatments were administered at a dosage of 1 mL/100 g body weight twice daily for 5 consecutive days. One hour after the final dose, the rats were anaesthetized, and abdominal aorta blood was collected. Serum was isolated via centrifugation, sterile-filtered, aliquoted, and stored at –80 °C for subsequent use.

Preparation of Drug-Containing Serum

Six experimental groups were established for serum collection: Control, OVX, CIA, OVX + CIA, OVX + CIA + EV, and OVX + CIA + YSJB (the Control, OVX, and CIA groups were treated as described in "Ovariectomy and Induction of Collagen-Induced Arthritis"). Nonarthritic rats were excluded 14 days after the primary immunization. The remaining OVX + CIA rats were randomly stratified into OVX + CIA, OVX + CIA + EV, and OVX + CIA + YSJB groups on the basis of joint swelling severity. Treatments commenced as follows: Control, OVX, CIA, and OVX + CIA groups: vehicle (purified water, p.o.); OVX + CIA + YSJB group: YSJB aqueous solution (0.3 g/mL, p.o.); and OVX + CIA + EV group: oestradiol valerate (EV) aqueous solution (0.0184 mg/mL, p.o.). All treatments were administered twice daily for 5 consecutive days at a dosage of 1 mL/100 g body weight. One hour after the final administration, the rats were anaesthetized, and blood was collected via abdominal aorta puncture. Serum was separated by centrifugation, sterile-filtered, aliquoted, and stored at –80 °C.

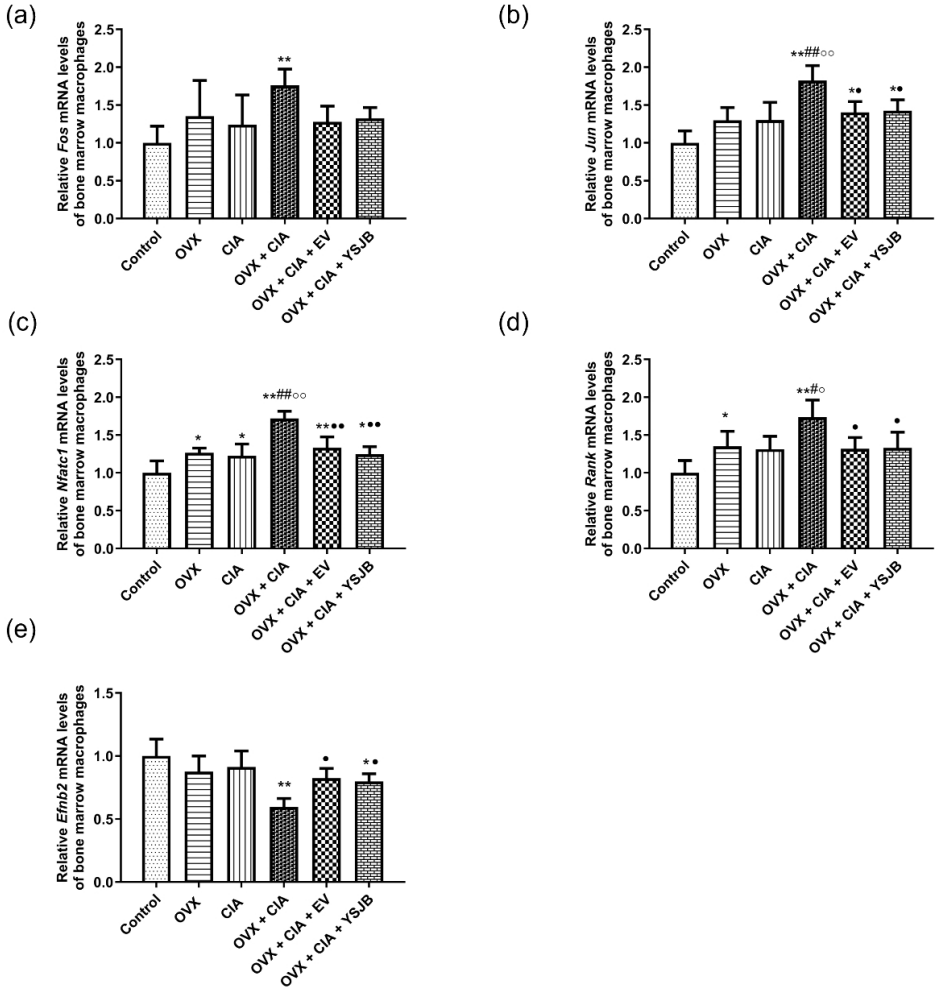

Fig. 4. YSJB upregulates *Efnb2* mRNA expression and inhibits osteoclast-related transcription factor expression in bone marrow-derived osteoclasts. (**a**) *c-Fos* mRNA expression, (**b**) *c-Jun* mRNA expression, (**c**) *Nfatc1* mRNA expression, (**d**) *Rank* mRNA expression, and (**e**) *Efnb2* mRNA expression. Statistical comparisons: $^{*}p < 0.05$, $^{**}p < 0.01$ vs. the Control group; $^{\#}p < 0.05$, $^{\#\#}p < 0.01$ vs. the OVX group; $^{\circ}p < 0.05$, $^{\circ\circ}p < 0.01$ vs. the CIA group; $^{\bullet}p < 0.05$, $^{\bullet\bullet}p < 0.01$ vs. the OVX + CIA group.

Osteoclast Differentiation and the Addition of Drug-Containing Serum

Induction and Differentiation of Osteoclasts from Spleen-Derived Monocytes

Ten female C57BL/6 mice (7–8 weeks old, 18–22 g) were euthanized under anaesthesia. Their spleens were subsequently harvested, rinsed, minced, homogenized, and then filtered through a cell strainer to obtain single-cell suspensions, followed by red blood cell lysis. The cells were resuspended in alpha minimum essential medium (α-MEM) (Gibco, Grand Island, NY, USA; C12571500BT) supplemented with 10 % foetal bovine serum (FBS) (Gibco, Grand Island, NY, USA; 10099-141) and adjusted to the target concentrations. Cells were plated at 5×10^5 cells/well in 96-well plates (with or without preloaded bone slices) or 3×10^6 cells/well in 24-well plates and then incubated at 37 °C with 5 % CO_2. After a 2-hour adhesion period, the medium was replaced with differentiation medium containing 25 ng/mL M-CSF (R&D, Minneapolis, MN, USA; 416-ML-010) and 50 ng/mL RANKL (PeproTech, Cranbury, NJ, USA, 400-30-10). Five days after plating, serum from the Control, OVX, CIA, OVX + CIA, OVX + CIA + EV, and OVX + CIA + YSJB groups was added to the cultures at a final serum concentration of 5 %.

Induction and Differentiation of Osteoclasts from BMMs

Twenty female C57BL/6 (7–8 weeks old, 18–22 g) mice were euthanized under anaesthesia. The tibias and femurs were subsequently isolated in a sterile culture dish and repeatedly rinsed. The epiphyseal ends of the bones were excised using sterile scissors, and the bone marrow cavity was repeatedly flushed ($\geq$3 times) with sterile phosphate-buffered saline (PBS) (Hyclone, Logan, UT, USA, SH30256.01). The collected bone marrow cell suspension was filtered through a cell strainer, followed by red blood cell lysis. Cells were resuspended in complete medium (α-MEM supplemented with 10 % FBS) and seeded in culture flasks for 24 hour at 37 °C with 5 % CO_2.

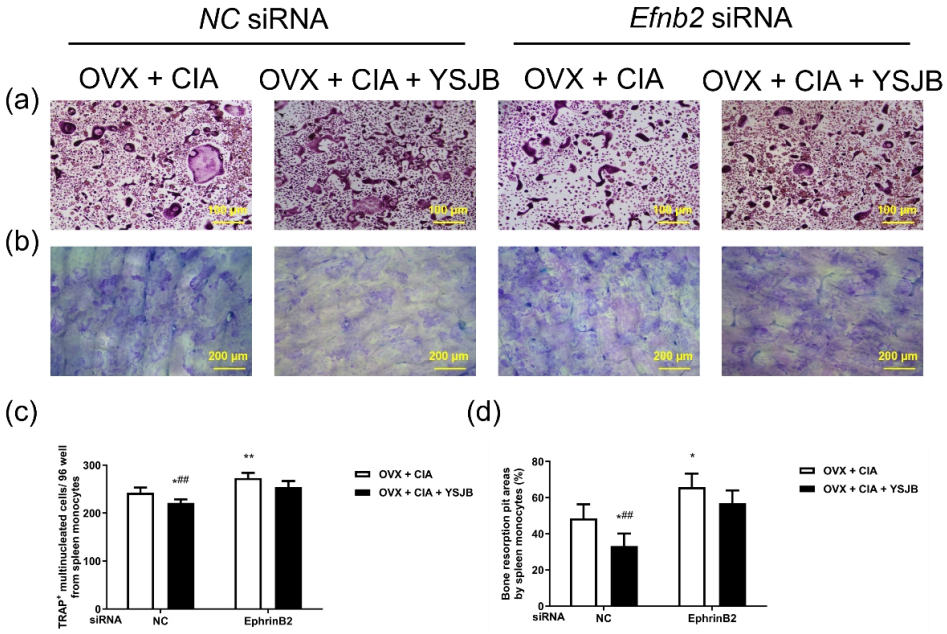

Fig. 5. Silencing *Efnb2* mRNA attenuated the inhibitory effects of YSJB in spleen-derived OCs (TRAP staining) and bone resorption activity (toluidine blue staining). (**a**) OC differentiation in the NC siRNA + OVX + CIA, NC siRNA + OVX + CIA + YSJB, *Efnb2* siRNA + OVX + CIA, and *Efnb2* siRNA + OVX + CIA + YSJB groups. The scale bar represents 100 μm. (**b**) Bone resorption activity in the NC siRNA + OVX + CIA, NC siRNA + OVX + CIA + YSJB, *Efnb2* siRNA + OVX + CIA, and *Efnb2* siRNA + OVX + CIA + YSJB groups. The scale bar represents 200 μm. (**c**) Quantitative changes in the number of spleen-derived OCs after *Efnb2* mRNA silencing. (**d**) Quantitative changes in the bone erosion area caused by spleen-derived OCs after *Efnb2* mRNA silencing. Statistical comparisons: $^{*}p < 0.05$, $^{**}p < 0.01$ vs. the NC siRNA + OVX + CIA group; $^{\#\#}p < 0.01$ vs. the *Efnb2* siRNA + OVX + CIA group.

Nonadherent cells were collected and adjusted to the target concentration in complete medium supplemented with 25 ng/mL M-CSF. Cells were plated at 5×10^4 cells/well in 96-well plates (with or without preloaded bone slices) or at 3×10^5 cells/well in 24-well plates, followed by incubation. Three days after plating, the medium was replaced with osteoclastogenic differentiation medium (25 ng/mL M-CSF + 50 ng/mL RANKL). On day 5 postplating, drug-containing serum from the Control, OVX, CIA, OVX + CIA, OVX + CIA + EV, and OVX + CIA + YSJB groups was added to each well at a final serum concentration of 5 %.

Transfection of Osteoclasts with Encoding EphrinB2 (Efnb2)-Targeted Small Interfering RNA (siRNA)

To assess the role of EphrinB2 in the efficacy of YSJB, four groups were established: negative control (NC) siRNA + OVX + CIA, *Efnb2* siRNA + OVX + CIA, NC siRNA + OVX + CIA + YSJB, and *EphrinB2* siRNA + OVX + CIA + YSJB. *Efnb2*-targeted siRNA was synthesized by Beijing Hesheng Biotechnology (Beijing, China, RX010990), with the following primer sequence (5′–3′): GCACAAUUAAGGAGAATT. Transfection was performed on day 5 postplating using Rfect Small Nucleic Acid Transfection Reagent (Changzhou Baidai Biotechnology, Changzhou, China, 11015, EXP: 202011). After 6 hours of transfection, the medium was replaced with fresh differentiation medium (25 ng/mL M-CSF + 50 ng/mL RANKL), and drug-containing serum from each group was added to a final serum concentration of 5 %.

Tartrate-Resistant Acid Phosphatase (TRAP) Staining

On day 7 postplating, osteoclasts were stained with a TRAP staining kit (Sigma, St. Louis, MO, USA; 387A-1KT). $TRAP^+$ multinucleated cells containing $\geq$3 nuclei were considered osteoclasts. The samples were examined under a Leica microscope (Leica, Wetzlar, Germany, CTR6000). For each group, we utilized three replicate wells and calculated the average number of osteoclasts.

Pit Formation Assay

On day 11 postplating, bone slices were transferred to a 24-well plate containing 0.25 mol/L ammonia hydroxide solution and cleaned via ultrasonic treatment. After air-drying, the slices were stained with 1 % toluidine blue staining solution for 10 min and rinsed with distilled water. The bone resorption pit area was analysed by light microscopy and quantified using a Leica Qwin (V3.5.0, Wetzlar, Germany).

Quantitative Reverse Transcription PCR (RT-qPCR) Analysis

On day 7 postplating, total RNA was extracted using TRIzol Reagent (Ambion, Austin, TX, USA, 15596026).

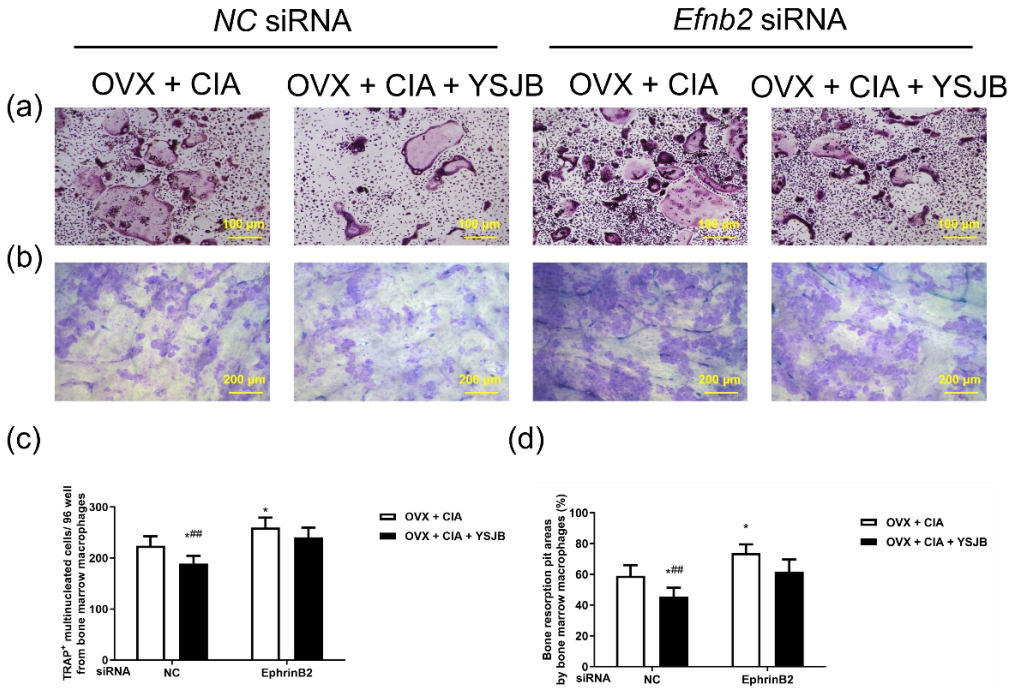

Fig. 6. Silencing *Efnb2* mRNA attenuated the inhibitory effects of YSJB in bone marrow-derived OCs (TRAP staining) and bone resorption activity (toluidine blue staining). (**a**) OC differentiation in the NC siRNA + OVX + CIA, NC siRNA + OVX + CIA + YSJB, *Efnb2* siRNA + OVX + CIA, and *Efnb2* siRNA + OVX + CIA + YSJB groups. The scale bar represents 100 μm. (**b**) Bone resorption activity in the NC siRNA + OVX + CIA, NC siRNA + OVX + CIA + YSJB, *Efnb2* siRNA + OVX + CIA, and *Efnb2* siRNA + OVX + CIA + YSJB groups. The scale bar represents 200 μm. (**c**) Quantitative changes in the number of spleen-derived OCs after *Efnb2* mRNA silencing. (**d**) Quantitative changes in the bone erosion area caused by spleen-derived OCs after *Efnb2* mRNA silencing. Statistical comparisons: $^{*}p < 0.05$ vs. the NC siRNA + OVX + CIA group; $^{\#\#}p < 0.01$ vs. the *Efnb2* siRNA + OVX + CIA group.

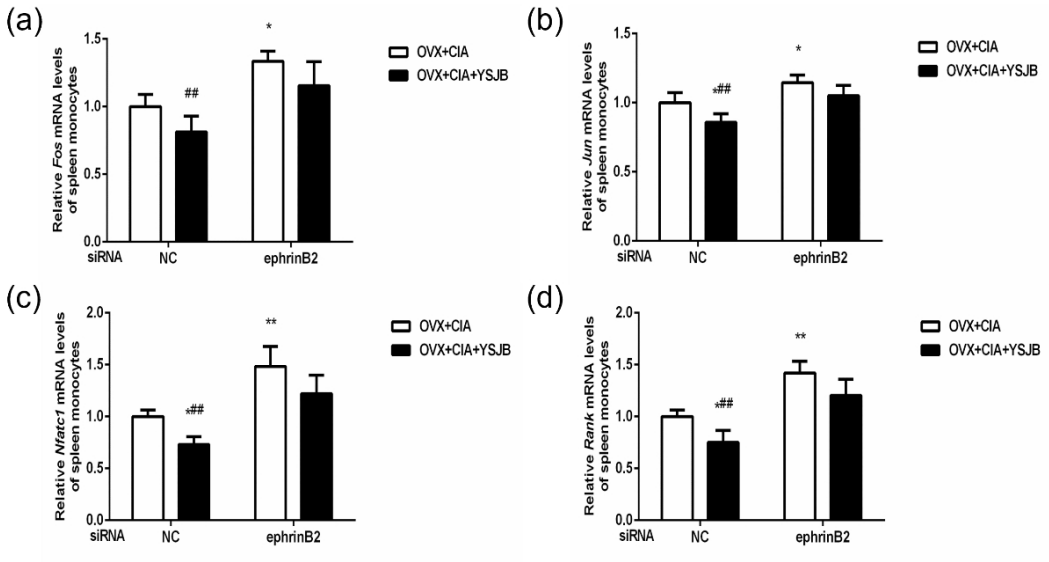

Fig. 7. Silencing *Efnb2* mRNA attenuates the inhibitory effects of YSJB on osteoclast-related transcription factor expression in spleen-derived osteoclasts. (**a**) Changes in *c-Fos* mRNA expression in spleen-derived osteoclasts. (**b**) Changes in c-Jun mRNA expression in spleen-derived osteoclasts. (**c**) Changes in *Nfatc1* mRNA expression in spleen-derived osteoclasts. (**d**) Changes in *Rank* mRNA expression in spleen-derived osteoclasts. Statistical comparisons: $^{*}p < 0.05$, $^{**}p < 0.01$ vs. the NC siRNA + OVX + CIA group. $^{\#\#}p < 0.01$ vs. the *Efnb2* siRNA + OVX + CIA group.

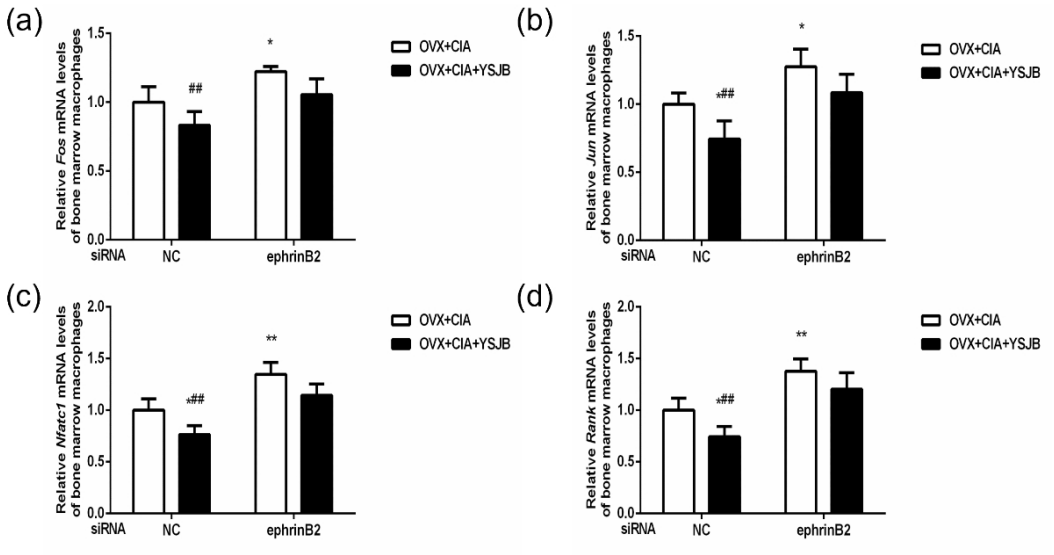

Fig. 8. Silencing *Efnb2* mRNA attenuates the inhibitory effects of YSJB on osteoclast-related transcription factor expression in bone marrow-derived osteoclasts. (**a**) Changes in *c-Fos* mRNA expression in spleen-derived osteoclasts. (**b**) Changes in *c-Jun* mRNA expression in spleen-derived osteoclasts. (**c**) Changes in *Nfatc1* mRNA expression in spleen-derived osteoclasts. (**d**) Changes in *Rank* mRNA expression in spleen-derived osteoclasts. Statistical comparisons: $^{*}p < 0.05$, $^{**}p < 0.01$ vs. the NC siRNA + OVX + CIA group; $^{\#\#}p < 0.01$ vs. the *Efnb2* siRNA + OVX + CIA group.

Reverse transcription and RT-qPCR were performed with Takara kits (Takara, Kumamoto, Japan; RR430A and RR036A). The primers used were synthesized by Sangon Biotech (Shanghai, China), and the sequences are listed in Table 1. The reaction was performed as follows: 30 s of predenaturation at 95 °C, followed by 40 cycles of 5 s of denaturation at 95 °C and 10 s of annealing at 60 °C. Gene expression was normalized to that of *GAPDH*, and relative expression was determined using the $2^{-\Delta\Delta Ct}$ method.

Statistical Analysis

Statistical analysis was performed using SPSS 24.0 software (IBM, Armonk, NY, USA). Data are presented as the mean ± standard deviation ($\bar{x} \pm$ SD). All experiments were performed with n = 3 biological replicates per group. Data normality was first assessed using the Shapiro–Wilk test. For normally distributed data, multigroup comparisons were made by one-way ANOVA, with post hoc pairwise comparisons conducted using the least significant difference (LSD) test for homogeneous variances or Dunnett's T3 test for heterogeneous variances. For nonnormally distributed data, the Kruskal–Wallis test was employed for multigroup comparisons, followed by stepwise step-down tests for pairwise comparisons. Statistical significance was defined as $p < 0.05$, with $p < 0.01$ indicating high significance.

Results

YSJB Inhibits Spleen and Bone Marrow Cell Differentiation into OCs and Bone Resorption Activity

In the context of spleen-derived OC differentiation, compared with the Control group, the OVX + CIA group and OVX group exhibited more OCs ($p = 0.002$, $p = 0.041$), whereas the CIA groups showed only nonsignificant increases in OC numbers ($p = 0.147$). Critically, compared with OVX + CIA, treatment with EV and YSJB significantly attenuated this osteoclastogenic response, reducing the number of OCs ($p = 0.039$, $p = 0.014$) (Fig. 1**a,c**). Toluidine blue staining revealed pathological bone resorption patterns: both the OVX ($p = 0.039$) and OVX + CIA ($p < 0.001$) groups exhibited resorption pits that were significantly larger than those in the Control group, whereas the pits in the CIA with Control groups were not significantly different ($p = 0.205$). Notably, the OVX + CIA + EV ($p = 0.012$) and OVX + CIA + YSJB ($p = 0.037$) groups demonstrated effective reversal of bone destruction and significantly reduced resorption areas compared with the OVX + CIA group (Fig. 1**b,d**).

In terms of bone marrow-derived OC differentiation, the OVX + CIA ($p = 0.003$) group presented significantly more OCs than the Control group did, whereas the numbers of OCs in the OVX and CIA groups did not significantly increase ($p = 0.075$, $p = 0.151$). Importantly, compared with OVX + CIA, both EV and YSJB treatment significantly suppressed osteoclastogenesis ($p = 0.025$, $p = 0.038$) (Fig. 2**a,c**). Quantification of the resorption pit area confirmed this result: the OVX ($p = 0.015$) and OVX + CIA ($p < 0.001$) groups exhibited significantly expanded

resorption areas compared with those of the Control. Conversely, compared with the OVX + CIA group, the therapeutic groups demonstrated significant bone protection, with a reduction in resorption (EV $p = 0.017$, YSJB $p = 0.004$) (Fig. 2**b,d**).

YSJB Upregulates Efnb2 Messenger RNA (mRNA) and Inhibits Osteoclast-Related Transcription Factor Expression in Spleen- and Bone Marrow-Derived Osteoclasts

Analysis of spleen-derived osteoclasts revealed distinct transcriptional patterns. Compared with that in the Control group, the mRNA expression of the osteoclastogenic transcription factor *c-Fos* significantly increased in the OVX + CIA group ($p = 0.006$), whereas the mRNA expression of *c-Fos* in both the OVX and CIA groups tended to increase, but the difference was not significant ($p = 0.098$, $p = 0.387$) (Fig. 3**a**). Similarly, transcription factor c-Jun (*c-Jun*) expression was markedly higher in the OVX + CIA group than in the Control ($p < 0.001$), OVX ($p = 0.002$) and CIA ($p = 0.003$) groups (Fig. 3**b**). *Nfatc1* expression was significantly upregulated in the OVX ($p = 0.023$), CIA ($p = 0.035$), and OVX + CIA ($p < 0.001$) groups compared with that in the Control group (Fig. 3**c**). Receptor activator of nuclear factor-κb (*Rank*) mRNA expression was significantly greater in the OVX + CIA group than in the Control ($p < 0.001$), OVX ($p = 0.008$) and CIA groups ($p = 0.005$) (Fig. 3**d**). Critically, *Efnb2* exhibited the opposite trend, and its expression was significantly lower in the OVX + CIA group than in the Control group ($p = 0.002$); furthermore, *Efnb2* expression in the OVX ($p = 0.111$) and CIA ($p = 0.127$) groups was lower, but the difference was not significant (Fig. 3**e**). The therapeutic interventions demonstrated consistent bidirectional effects: osteoclast markers were significantly decreased in both the OVX + CIA + EV and OVX + CIA + YSJB groups compared with those in the OVX + CIA group (*c-Jun*: YSJB $p = 0.048$; *Nfatc1*: EV $p = 0.011$; YSJB $p = 0.004$; *Rank*: EV $p = 0.008$; YSJB $p = 0.022$) but *Efnb2* expression increased (EV $p = 0.040$; YSJB $p = 0.011$) (Fig. 3**a–e**).

In bone marrow-derived osteoclasts, parallel regulatory patterns emerged. The OVX + CIA group exhibited upregulation of *c-Fos* ($p = 0.009$ vs. Control; $p = 0.173$ vs. OVX; $p = 0.342$ vs. CIA) (Fig. 4**a**), *c-Jun* ($p < 0.001$ vs. Control; $p = 0.004$ vs. OVX; $p = 0.004$ vs. CIA) (Fig. 4**b**), *Nfatc1* ($p < 0.001$ vs. Control; $p < 0.001$ vs. OVX; $p < 0.001$ vs. CIA), (Fig. 4**c**) and *Rank* ($p < 0.001$ vs. Control; $p = 0.028$ vs. OVX; $p = 0.012$ vs. CIA) (Fig. 4**d**). Consistent with the spleen cell observations, *Efnb2* expression was significantly lower in the OVX + CIA group than in the Control group ($p < 0.001$) (Fig. 4**e**). Both therapeutic regimens effectively reversed these pathological changes: the expression of osteoclast transcription factors was significantly reduced in the OVX + CIA + EV and OVX + CIA + YSJB groups compared with that in the OVX + CIA group (*c-Jun*: EV $p = 0.013$, YSJB $p = 0.018$; *Nfatc1*: EV $p = 0.003$, YSJB $p < 0.001$; *Rank*: EV $p = 0.019$, YSJB $p = 0.022$) while *Efnb2* expression was restored compared with that in the OVX + CIA group (EV $p = 0.019$, YSJB $p = 0.034$) (Fig. 4**a–e**). This coordinated inverse relationship between the expression of *Efnb2* and osteoclastogenic factors across cellular sources suggests that *Efnb2* serves as a central regulatory node mediating the antiresorptive effects of YSJB.

Silencing Efnb2 mRNA Attenuates the Inhibitory Effects of YSJB on OC Differentiation and Bone Resorption Activity

Efnb2 was silenced in spleen-derived osteoclasts via *Efnb2*-targeted siRNA transfection, after which the *Efnb2* siRNA + OVX + CIA group exhibited a significant increase in the number of OCs compared with that in the NC siRNA + OVX + CIA group ($p = 0.008$), whereas the number of OCs in the NC siRNA + OVX + CIA + YSJB group significantly decreased ($p = 0.044$). Compared with the *Efnb2* siRNA + OVX + CIA group, the *Efnb2* siRNA + OVX + CIA + YSJB group showed a decreasing trend in OC numbers ($p = 0.067$) (Fig. 5**a,c**). Toluidine blue staining revealed that the bone resorption pit areas in the *Efnb2* siRNA + OVX + CIA group were significantly larger than those in the NC siRNA + OVX + CIA group ($p = 0.021$), whereas the pit areas in the NC siRNA + OVX + CIA + YSJB group were significantly reduced ($p = 0.034$). Compared with the *Efnb2* siRNA + OVX + CIA group, the *Efnb2* siRNA + OVX + CIA + YSJB group exhibited a decreasing trend in bone resorption pit area ($p = 0.179$) (Fig. 5**b,d**).

The silencing of *Efnb2* in bone marrow-derived osteoclasts resulted in similar trends. The *Efnb2* siRNA + OVX + CIA group had significantly more OCs than the NC siRNA + OVX + CIA group did ($p = 0.043$), the OC numbers in the NC siRNA + OVX + CIA + YSJB group were significantly lower ($p = 0.048$). Compared with the *Efnb2* siRNA + OVX + CIA group, the *Efnb2* siRNA + OVX + CIA + YSJB group showed a decreasing trend in OC numbers ($p = 0.237$) (Fig. 6**a,c**). Toluidine blue staining indicated that bone resorption pit areas in the *Efnb2* siRNA + OVX + CIA group were significantly larger than those in the NC siRNA + OVX + CIA group ($p = 0.027$), with the NC siRNA + OVX + CIA + YSJB group showing smaller pit areas ($p = 0.037$). A decreasing trend in pit areas was observed in the *Efnb2* siRNA + OVX + CIA + YSJB group compared with the *Efnb2* siRNA + OVX + CIA group ($p = 0.057$) (Fig. 6**b,d**).

Silencing Efnb2 mRNA Attenuates the Inhibitory Effects of YSJB on Osteoclast-Related Transcription Factor Expression

Analysis of spleen-derived osteoclasts revealed distinct transcriptional patterns. Compared with the NC siRNA + OVX + CIA group, the *Efnb2* siRNA + OVX + CIA group exhibited significant upregulation of osteoclast-related transcription factors, with increased *c-Fos* (Fig. 7**a**),

c-Jun (Fig. 7**b**), *Nfatc1*(Fig. 7**c**), and *Rank* (Fig. 7**d**) mRNA expression (*c-Fos*: $p = 0.010$, *c-Jun*: $p = 0.030$, *Nfatc1*: $p = 0.003$, *Rank*: $p = 0.002$). Compared with the NC siRNA + OVX + CIA group, the expression of *c-Jun*, *Nfatc1*, and *Rank* mRNA in the NC siRNA + OVX + CIA + YSJB group was effectively decreased (*c-Jun*: $p = 0.032$; *Nfatc1*: $p = 0.047$; *Rank*: $p = 0.031$), whereas the expression of *c-Fos* only tended to decrease ($p = 0.097$). Critically, under *Efnb2* silencing conditions, the regulatory efficacy of YSJB was lost, as the *Efnb2* siRNA + OVX + CIA + YSJB group demonstrated only decreasing trends for the expression all four transcription factors compared with the *Efnb2* siRNA + OVX + CIA group (*c-Fos*: $p = 0.109$, *c-Jun*: $p = 0.124$, *Nfatc1*: $p = 0.054$, *Rank*: $p = 0.052$).

Consistent with the spleen-derived osteoclast observations, the analysis of bone marrow-derived osteoclasts revealed that compared with the NC siRNA + OVX + CIA group, the *Efnb2* siRNA + OVX + CIA group showed significant upregulation of *c-Fos* (Fig. 8**a**), *c-Jun* (Fig. 8**b**), *Nfatc1* (Fig. 8**c**), and *Rank* (Fig. 8**d**) mRNA expression (*c-Fos*: $p = 0.023$, *c-Jun*: $p = 0.025$, *Nfatc1*: $p = 0.004$, *Rank*: $p = 0.006$). YSJB maintained efficacy in nonsilenced cells, significantly reducing *c-Jun*, *Nfatc1*, and *Rank* expression in the NC siRNA + OVX + CIA + YSJB group compared with that in the NC siRNA + OVX + CIA group (*c-Jun*: $p = 0.034$; *Nfatc1*: $p = 0.027$; *Rank*: $p = 0.038$), with *c-Fos* expression tending to decrease ($p = 0.066$). Notably, silencing *Efnb2* compromised the effects of YSJB, as the *Efnb2* siRNA + OVX + CIA + YSJB group showed decreasing trends for the expression of all transcription factors vs. the *Efnb2* siRNA + OVX + CIA group (*c-Fos*: $p = 0.065$; *c-Jun*: $p = 0.092$; *Nfatc1*: $p = 0.051$; *Rank*: $p = 0.130$).

Discussion

Postmenopausal women with RA frequently exhibit accelerated bone destruction, which is closely linked to oestrogen deficiency-induced bone metabolism disorders [32,33]. Oestrogen directly inhibits OC precursor differentiation, and oestrogen deficiency disrupts the balance of bone remodelling [34]. Beyond its direct detrimental effects on bone, estrogen deficiency primarily underlies persistent bone destruction via chronic low-grade inflammation, a process triggered by altered cytokine expression and dysfunctional immune responses [35]. Specific subsets of T lymphocytes expressing tumor necrosis factor-alpha (TNF-α) can increase osteoblast apoptosis and indirectly stimulate osteoclastogenesis via RANKL produced by B cells, triggering bone loss in postmenopausal osteoporosis [35]. Additionally, oestrogen directly inhibits bone resorption and maintains bone mass through its action on osteoclasts. 17β-estradiol (E2) counteracts RANKL-induced mitochondrial changes and promotes mitochondria-mediated apoptosis, further contributing to the regulation of bone homeostasis [36]. Low oestrogen status upregulates inflammatory cytokines such as TNF-α and IL-6 and further promotes osteoclastogenesis through the activation of the RANKL/RANK signalling pathway [35]. Moreover, bone marrow macrophages in postmenopausal women may drive pathological synergies between postmenopausal osteoporosis (PMOP) and RA through cytokine secretion [37].

OC precursors, which are primarily derived from bone marrow cells and monocytes, differentiate into mature OCs under M-CSF and RANKL induction. To comprehensively evaluate the regulatory effects of YSJB on OC differentiation under conditions mimicking bone loss with oestrogen deficiency in the context of RA, we employed two *in vitro* models: spleen-derived monocytes (simulating the joint inflammatory environment) and bone marrow-derived mononuclear macrophages (simulating the intraosseous destructive niche). Using drug-containing serum from ovariectomized (OVX) rats with collagen-induced arthritis (CIA) to mimic postmenopausal RA pathology, we observed significantly more OCs and increased bone resorption pit areas in both models compared with those in the Control and CIA groups ($p < 0.05$). These results confirm that ovariectomy exacerbates OC activation and bone destruction. Notably, YSJB intervention reversed these pathological changes, reducing OC numbers and resorption pit areas.

Mechanistically, the binding of RANKL to RANK activates downstream c-Fos and NFATc1, both of which are essential for osteoclastogenesis [38–40]. NFATc1, a master transcription factor for osteoclast differentiation, can induce osteoclast formation even in c-Fos-deficient precursors [41,42]. c-Jun, another transcription factor downstream of RANKL signalling, promotes NFATc1 expression once activated [43]. Notably, c-Jun combines with c-Fos to form the AP-1 transcription complex, which regulates OC survival and function [44]. Our prior work revealed that YSJB upregulates EphrinB2 expression in bone marrow cells, reducing OC numbers and NFATc1 expression in OVX + CIA rats. EphrinB2, a member of the Ephrin family, has been implicated in orthopaedic conditions [45,46]. *In vitro*, the novel vitamin D analogue eldecalcitol (ED-71) ameliorated H_2O_2-induced osteoporosis by inhibiting oxidative stress and suppressing osteoclastogenesis and osteoclast function via EphrinB2 upregulation; importantly, EphrinB2 knockdown reversed the inhibitory effects of ED-71 [47]. The EphB4/EphrinB2 signalling axis plays a pivotal role in bone remodelling. EphB4 forwards signalling promotes osteoblast differentiation, whereas EphrinB2 reverse signalling inhibits osteoclast formation by suppressing c-Fos/NFATc1 cascades [27]. In our study, *Efnb2* was downregulated in the OVX + CIA group, and *c-Fos*, *c-Jun*, *NFATc1*, and *RANK* were upregulated. YSJB treatment restored *Efnb2* levels and inhibited the expression of these pro-osteoclastogenic factors. Furthermore, *Efnb2* knockdown exacerbated osteoclast activation and increased *c-Fos*, *c-Jun*, *NFATc1*, and *RANK* expression in the OVX + CIA group, confirming the bone pro-

tective role of EphrinB2. Although YSJB partially reversed osteoclast activation after *Efnb2* knockdown (with a trend towards reduced *c-Fos* expression), its efficacy was attenuated, indicating that EphrinB2 is a critical target for the bone protective effects of YSJB.

The innovative aspects of this study include the systematic validation of the synergistic regulatory effects of YSJB-containing serum on osteoclast precursors derived from two distinct sources—the spleen and bone marrow—which simulate the inflammatory joint environment and the intraosseous destructive niche, respectively. These two-source precursor models offer a more comprehensive representation of pathological bone loss in individuals with postmenopausal RA than single-source approaches do. Moreover, the use of drug-containing serum from a disease model that integrates both ovariectomy and CIA provides a pharmacologically relevant platform for evaluating TCM interventions under conditions that mimic clinical postmenopausal RA. Crucially, we identified EphrinB2 as a necessary mediator of the inhibitory effect of YSJB on osteoclastogenesis, providing a previously uncharacterized molecular basis for the kidney-tonifying and bone-strengthening effects of this TCM in the context of RA with oestrogen deficiency. However, this study has several limitations. The conclusions are based primarily on results of TRAP staining, pit formation assays, and RT-qPCR for gene expression analysis. The lack of confirmation at the protein level by Western blotting or immunofluorescence limits the depth of mechanistic insight. In addition, only the *Efnb2* pathway was investigated; further inhibition or rescue experiments targeting other key molecules would strengthen causal inference. Although our previous *in vivo* studies confirmed that YSJB alleviates bone destruction in CIA and OVX + CIA rats, the current work lacks *in vivo* structural validation for direct correlation with the cellular findings. Larger sample sizes are also needed to enhance statistical robustness and generalizability.

According to the TCM principle of "kidney governing bone and marrow," kidney function is closely related to skeletal homeostasis, and kidney-tonifying herbs regulate bone remodelling by balancing bone resorption and formation [48,49]. Our earlier findings revealed that the therapeutic effect of YSJB is more pronounced in OVX + CIA rats, reflecting syndrome-specific pharmacology and the intrinsic link between TCM kidney deficiency syndrome and the postmenopausal state. This study highlights that the EphrinB2-mediated regulation of *c-Fos*, *c-Jun*, *Nfatc1*, and *RANK* expression in OC precursors from different sources (the spleen and bone marrow) is a key mechanism underlying accelerated bone destruction in postmenopausal patients with RA. These results also indicate that EphrinB2 is a critical molecular target for the kidney-tonifying effects of YSJB in individuals with RA. These findings underscore the potential of YSJB as an adjunctive therapy for managing the accelerated bone destruction that occurs in postmenopausal patients with RA. Given that conventional disease-modifying antirheumatic drugs and biologics primarily target inflammatory pathways, their direct impact on osteoclast activation driven by oestrogen deficiency may be limited. YSJB, rooted in the TCM principle that "the kidney governs bones and marrow", may offer a complementary strategy that specifically addresses the disrupted balance in bone remodelling in this vulnerable population. Future studies exploring the combination of YSJB with standard RA therapies such as methotrexate or anti-RANKL agents could reveal synergistic benefits, potentially by reducing the required dosage of biologics or mitigating their side effects. Furthermore, the identification of EphrinB2 as a key target opens avenues for the development of novel bone protective agents inspired by TCM formulations.

Conclusions

YSJB serum inhibits osteoclastogenesis in both bone marrow-derived macrophages and splenic monocytes. Our study revealed that YSJB serum exerts its effects by upregulating *Efnb2*, leading to reduced expression of *c-Fos*, *c-Jun*, *Nfatc1*, and *Rank* in OCs, thereby decreasing OC numbers and the bone resorption pit area. These results were confirmed by *Efnb2* knockdown experiments, in which the protective effects of YSJB serum were reversed. These findings provide new insights into the molecular mechanisms of YSJB and lay a theoretical foundation for the development of novel therapeutic strategies for treating individuals with postmenopausal rheumatoid arthritis.

List of Abbreviations

RA, rheumatoid arthritis; OCs, osteoclasts; EphrinB2, Eph receptor interacting protein B2; EphB4, Eph receptor B4; c-Fos, cellular oncogene c-Fos; NFATc1, nuclear factor of activated T cells cytoplasmic 1; TCM, traditional Chinese medicine; YSJB, Yishenjuanbi pill; OVX + CIA, ovariectomized collagen-induced arthritis; BMMs, bone marrow-derived macrophages; EV, oestradiol valerate; RT-qPCR, quantitative reverse transcription PCR; TRAP, tartrate-resistant acid phosphatase; c-Jun, transcription factor c-Jun; Rank, receptor activator of nuclear factor-κb; Efnb2, encoding EphrinB2; M-CSF, macrophage colony-stimulating factor; RANKL, receptor activator of nuclear factor-κB ligand; BV, bone volume; FBS, foetal bovine serum; ED-71, eldecalcitol; CT, computed tomography; IL, interleukin; HPLC, high performance liquid chromatography; SPF, specific pathogen free; α-MEM, alpha minimum essential medium; siRNA, small interfering RNA; NC, negative control; mRNA, messenger RNA; TNF-α, tumor necrosis factor-alpha.

Availability of Data and Materials

The datasets used and analysed during the current study were available from the corresponding author on reasonable request.

Author Contributions

HYZ, DPF and YSS contributed to the design and supervision of this work. JFC, HHX, HL, JHP and SJW performed experimental validation. YYW, JFC and HHX analyzed the data. HL, JHP, SJW and HRJ contributed to the interpretation of data. YYW drafted the work. YL, HHX, LT and HRJ revised critically for important intellectual content. All authors read and approved the final manuscript. All authors agreed to be accountable for all aspects of the work in ensuring that questions related to the accuracy or integrity of any part of the work were appropriately investigated and resolved.

Ethics Approval and Consent to Participate

The animal study protocol was approved by the Institutional Review Board of the Institute of Basic Theory of Traditional Chinese Medicine, China Academy of Chinese Medical Sciences (protocol code 2016-030).

Acknowledgments

Not applicable.

Funding

This work was funded by the National Natural Science Foundation of China under Grant (82074299, 82405039, 82305017), the Fundamental Research Funds for the Central Public Welfare Research Institutes under Grant (XTCX2023003), and the Shenzhen Science and Technology Program under Grant (JCYJ20240813152436047).

Conflict of Interest

The authors declare no conflict of interest.

References

[1] Gravallese EM, Firestein GS. Rheumatoid Arthritis-Common Origins, Divergent Mechanisms. The New England Journal of Medicine. 2023; 388: 529–542. http://doi.org/10.1056/NEJMra2103726.

[2] Ma Y, Chen H, Lv W, Wei S, Zou Y, Li R, *et al*. Global, regional and national burden of rheumatoid arthritis from 1990 to 2021, with projections of incidence to 2050: a systematic and comprehensive analysis of the Global Burden of Disease study 2021. Biomarker Research. 2025; 13: 47. https://doi.org/10.1186/s40364-025-00760-8.

[3] Förger F, Villiger PM. Immunological adaptations in pregnancy that modulate rheumatoid arthritis disease activity. Nature Reviews. Rheumatology. 2020; 16: 113–122. http://doi.org/10.1038/s41584-019-0351-2.

[4] Kim HN, Ponte F, Nookaew I, Ucer Ozgurel S, Marques-Carvalho A, Iyer S, *et al*. Estrogens decrease osteoclast number by attenuating mitochondria oxidative phosphorylation and ATP production in early osteoclast precursors. Scientific Reports. 2020; 10: 11933. https://doi.org/10.1038/s41598-020-68890-7.

[5] Xu H, Tao L, Cao J, Zhang P, Zeng H, Zhao H. Yi Shen Juan Bi Pill alleviates bone destruction in inflammatory arthritis under postmenopausal conditions by regulating ephrinB2 signaling. Frontiers in Pharmacology. 2022; 13: 1010640. https://doi.org/10.3389/fphar.2022.1010640.

[6] Mansoori MN, Raghuvanshi A, Shukla P, Awasthi P, Trivedi R, Goel A, *et al*. Medicarpin prevents arthritis in post-menopausal conditions by arresting the expansion of TH17 cells and pro-inflammatory cytokines. International Immunopharmacology. 2020; 82: 106299. http://doi.org/10.1016/j.intimp.2020.106299.

[7] Komatsu N, Takayanagi H. Mechanisms of joint destruction in rheumatoid arthritis-immune cell-fibroblast-bone interactions. Nature Reviews. Rheumatology. 2022; 18: 415–429. http://doi.org/10.1038/s41584-022-00793-5.

[8] Allard-Chamard H, Carrier N, Dufort P, Durand M, de Brum-Fernandes AJ, Boire G, *et al*. Osteoclasts and their circulating precursors in rheumatoid arthritis: Relationships with disease activity and bone erosions. Bone Reports. 2020; 12: 100282. http://doi.org/10.1016/j.bonr.2020.100282.

[9] Remmers S, Mayer D, Melke J, Ito K, Hofmann S. Measuring mineralised tissue formation and resorption in a human 3D osteoblast-osteoclast co-culture model. European Cells & Materials. 2020; 40: 189–202. https://doi.org/10.22203/eCM.v040a12.

[10] Yokota K. Osteoclast differentiation in rheumatoid arthritis. Immunological Medicine. 2024; 47: 6–11. http://doi.org/10.1080/25785826.2023.2220931.

[11] Yang Y, Liu Z, Wu J, Bao S, Wang Y, Li J, *et al*. Nrf2 Mitigates RANKL and M-CSF Induced Osteoclast Differentiation via ROS-Dependent Mechanisms. Antioxidants. 2023; 12: 2094. https://doi.org/10.3390/antiox12122094.

[12] Qi G, Jiang Z, Lu W, Li D, Chen W, Yang X, *et al*. Berbamine inhibits RANKL- and M-CSF-mediated osteoclastogenesis and alleviates ovariectomy-induced bone loss. Frontiers in Pharmacology. 2022; 13: 1032866. https://doi.org/10.3389/fphar.2022.1032866.

[13] Tang K, Deng W, Huang Z, Chen S, Zhu Z, Lin S, *et al*. Neoandrographolide inhibits mature osteoclast differentiation to alleviate bone loss and treat osteoporosis. Frontiers in Pharmacology. 2025; 16: 1466057. https://doi.org/10.3389/fphar.2025.1466057.

[14] Bae S, Kim K, Kang K, Kim H, Lee M, Oh B, *et al*. RANKL-responsive epigenetic mechanism reprograms macrophages into bone-resorbing osteoclasts. Cellular & Molecular Immunology. 2023; 20: 94–109. https://doi.org/10.1038/s41423-022-00959-x.

[15] Hascoët E, Blanchard F, Blin-Wakkach C, Guicheux J, Lesclous P, Cloitre A. New insights into inflammatory osteoclast precursors as therapeutic targets for rheumatoid arthritis and periodontitis. Bone Research. 2023; 11: 26. https://doi.org/10.1038/s41413-023-00257-w.

[16] Yun HM, Kim B, Kim E, Park KR. Rhusflavone Modulates Osteoclastogenesis Through RANKL-Induced AKT Signaling in Bone Marrow-Derived Macrophages. International Journal of Molecular Sciences. 2025; 26: 3025. https://doi.org/10.3390/ijms26073025.

[17] Jiang T, Su S, Tian R, Jiao Y, Zheng S, Liu T, *et al*. Immunoregulatory orchestrations in osteoarthritis and mesenchymal stromal cells for therapy. Journal of Orthopaedic Translation. 2025; 55: 38–54. http://doi.org/10.1016/j.jot.2025.08.009.

[18] Henning P, Movérare-Skrtic S, Westerlund A, Chaves de Souza PP, Floriano-Marcelino T, Nilsson KH, *et al*. WNT16 is Robustly Increased by Oncostatin M in Mouse Calvarial Osteoblasts and Acts as a Negative Feedback Regulator of Osteoclast Formation Induced by Oncostatin M. Journal of Inflammation Research. 2021; 14: 4723–4741. https://doi.org/10.2147/jir.S323435.

[19] Ray S, McCall JL, Tian JB, Jeon J, Douglas A, Tyler K, *et al*. Targeting TRPC channels for control of arthritis-induced bone erosion. Science Advances. 2025; 11: eabm9843. http://doi.org/10.1126/sciadv.abm9843.

[20] Cai X, Li Z, Zhao Y, Katz J, Michalek SM, Feng X, *et al*. Enhanced dual function of osteoclast precursors following calvarial Porphyromonas gingivalis infection. Journal of Periodontal Research. 2020; 55: 410–425. https://doi.org/10.1111/jre.12725.

[21] Di Ceglie I, van Lent PLEM, Geven EJW, Koenders MI, Blom AB, Vogl T, *et al*. S100A8/A9 is not essential for the development of inflammation and joint pathology in interleukin-1 receptor antagonist knockout mice. Arthritis Research & Therapy. 2021; 23: 216. http://doi.org/10.1186/s13075-021-02602-y.

[22] Piffko A, Uhl C, Vajkoczy P, Czabanka M, Broggini T. EphrinB2-EphB4 Signaling in Neurooncological Disease. International Journal of Molecular Sciences. 2022; 23: 1679. https://doi.org/10.3390/ijms23031679.

[23] Guo S, Wang Y, Duan Q, Gu W, Fu Q, Ma Z, *et al*. Activation of EphrinB2/EphB2 signaling in the spine cord alters glia-neuron interactions in mice with visceral hyperalgesia following maternal separation. Frontiers in Pharmacology. 2024; 15: 1463339. https://doi.org/10.3389/fphar.2024.1463339.

[24] Psilopatis I, Souferi-Chronopoulou E, Vrettou K, Troungos C, Theocharis S. EPH/Ephrin-Targeting Treatment in Breast Cancer: A New Chapter in Breast Cancer Therapy. International Journal of Molecular Sciences. 2022; 23: 15275. https://doi.org/10.3390/ijms232315275.

[25] Li T, Wang H, Liu R, Wang X, Huang L, Wu Z, *et al*. The role of EphB4/ephrinB2 signaling in root repair after orthodontically-induced root resorption. American Journal of Orthodontics and Dentofacial Orthopedics: Official Publication of the American Association of Orthodontists, its Constituent Societies, and the American Board of Orthodontics. 2021; 159: e217–e232. http://doi.org/10.1016/j.ajodo.2020.07.035.

[26] Fu Y, Zhang S, Liu J, Lu Z, Li Y, Liu J, *et al*. Imbalanced EphB4/EphrinB2 Signaling Modulates Bone Resorption in Periodontitis Induced by *Porphyromonas gingivalis*. ACS Infectious Diseases. 2024; 10: 1152–1161. https://doi.org/10.1021/acsinfecdis.3c00459.

[27] Zhao C, Irie N, Takada Y, Shimoda K, Miyamoto T, Nishiwaki T, *et al*. Bidirectional ephrinB2-EphB4 signaling controls bone homeostasis. Cell Metabolism. 2006; 4: 111–121. http://doi.org/10.1016/j.cmet.2006.05.012.

[28] Park G, Moon JH, Park SH, Kim JH, Seo BK, Lee SD, *et al*. The Effectiveness and Safety of Yi Shen Juan Bi Pill on Rheumatoid Arthritis: a Protocol for Systematic Review and/or Meta-Analysis. Journal of Acupuncture and Meridian Studies. 2024; 17: 116–122. http://doi.org/10.51507/j.jams.2024.17.4.116.

[29] Chang G, Qingwen T, Haoying YI, Yuting B, Jianming W. Network Meta-analysis of the clinical efficacy and safety of kidney-tonifying and bone-strengthening therapies for the treatment of rheumatoid arthritis with kidney deficiency type. Journal of Traditional Chinese Medicine = Chung I Tsa Chih Ying Wen Pan/Sponsored by All-China Association of Traditional Chinese Medicine, Academy of Traditional Chinese Medicine. 2024; 44: 1067–1081. https://doi.org/10.19852/j.cnki.jtcm.20240927.002.

[30] Guo ZH, Ni HY, Tang MY. Clinical efficacy and pharmacological mechanism analysis of Xubi Capsule in the treatment of patients with liver and kidney deficiency osteoarthritis. Medicine. 2024; 103: e39327. http://doi.org/10.1097/MD.0000000000039327.

[31] Xia Y, Fan D, Li X, Lu X, Ye Q, Xi X, *et al*. Yi Shen Juan Bi Pill Regulates the Bone Immune Microenvironment via the JAK2/STAT3 Signaling Pathway *in Vitro*. Frontiers in Pharmacology. 2021; 12: 746786. https://doi.org/10.3389/fphar.2021.746786.

[32] Hsu SH, Chen LR, Chen KH. Primary Osteoporosis Induced by Androgen and Estrogen Deficiency: The Molecular and Cellular Perspective on Pathophysiological Mechanisms and Treatments. International Journal of Molecular Sciences. 2024; 25: 12139. https://doi.org/10.3390/ijms252212139.

[33] Gómez-Vaquero C, Hernández JL, Olmos JM, Cerdà D, Calleja CH, López JAM, *et al*. High incidence of clinical fragility fractures in postmenopausal women with rheumatoid arthritis. A case-control study. Bone. 2023; 168: 116654. http://doi.org/10.1016/j.bone.2022.116654.

[34] Cheng CH, Chen LR, Chen KH. Osteoporosis Due to Hormone Imbalance: An Overview of the Effects of Estrogen Deficiency and Glucocorticoid Overuse on Bone Turnover. International Journal of Molecular Sciences. 2022; 23: 1376. https://doi.org/10.3390/ijms23031376.

[35] Fischer V, Haffner-Luntzer M. Interaction between bone and immune cells: Implications for postmenopausal osteoporosis. Seminars in Cell & Developmental Biology. 2022; 123: 14–21. http://doi.org/10.1016/j.semcdb.2021.05.014.

[36] Marques-Carvalho A, Sardão VA, Kim HN, Almeida M. ECSIT is essential for RANKL-induced stimulation of mitochondria in osteoclasts and a target for the anti-osteoclastogenic effects of estrogens. Frontiers in Endocrinology. 2023; 14: 1110369. https://doi.org/10.3389/fendo.2023.1110369.

[37] Xu Y, Yan H, Zhang X, Zhuo J, Han Y, Zhang H, *et al*. Roles of Altered Macrophages and Cytokines: Implications for Pathological Mechanisms of Postmenopausal Osteoporosis, Rheumatoid Arthritis, and Alzheimer's Disease. Frontiers in Endocrinology. 2022; 13: 876269. https://doi.org/10.3389/fendo.2022.876269.

[38] Jiang T, Xia T, Qiao F, Wang N, Jiang Y, Xin H. Role and Regulation of Transcription Factors in Osteoclastogenesis. International Journal of Molecular Sciences. 2023; 24: 16175. https://doi.org/10.3390/ijms242216175.

[39] Fujii T, Murata K, Mun SH, Bae S, Lee YJ, Pannellini T, *et al*. MEF2C regulates osteoclastogenesis and pathologic bone resorption via c-FOS. Bone Research. 2021; 9: 4. https://doi.org/10.1038/s41413-020-00120-2.

[40] Matsuoka K, Bakiri L, Bilban M, Toegel S, Haschemi A, Yuan H, *et al*. Metabolic rewiring controlled by c-Fos governs cartilage integrity in osteoarthritis. Annals of the Rheumatic Diseases. 2023; 82: 1227–1239. http://doi.org/10.1136/ard-2023-224002.

[41] Omata Y, Tachibana H, Aizaki Y, Mimura T, Sato K. Essentiality of Nfatc1 short isoform in osteoclast differentiation and its self-regulation. Scientific Reports. 2023; 13: 18797. https://doi.org/10.1038/s41598-023-45909-3.

[42] Stegen S, Moermans K, Stockmans I, Thienpont B, Carmeliet G. The serine synthesis pathway drives osteoclast differentiation through epigenetic regulation of NFATc1 expression. Nature Metabolism. 2024; 6: 141–152. https://doi.org/10.1038/s42255-023-00948-y.

[43] He F, Luo S, Liu S, Wan S, Li J, Chen J, *et al*. Zanthoxylum bungeanum seed oil inhibits RANKL-induced osteoclastogenesis by suppressing ERK/c-JUN/NFATc1 pathway and regulating cell cycle arrest in RAW264.7 cells. Journal of Ethnopharmacology. 2022; 289: 115094. http://doi.org/10.1016/j.jep.2022.115094.

[44] Yasuda K, Matsubara T, Shirakawa T, Kawamoto T, Kokabu S. Protein phosphatase 1 regulatory subunit 18 suppresses the transcriptional activity of NFATc1 via regulation of c-fos. Bone Reports. 2021; 15: 101114. http://doi.org/10.1016/j.bonr.2021.101114.

[45] Ge Y, Feng K, Liu X, Chen H, Sun Z, Wang C, *et al*. The Recombinant Protein EphB4-Fc Changes the Ti Particle-Mediated Imbalance of OPG/RANKL via EphrinB2/EphB4 Signaling Pathway and Inhibits the Release of Proinflammatory Factors *in Vivo*. Oxidative Medicine and Cellular Longevity. 2020; 2020: 1404915. http://doi.org/10.1155/2020/1404915.

[46] Yu H, Wei X, Jiang H, Qi H, Zhang Y, Hu M. Tensile force promotes osteogenic differentiation via ephrinB2-EphB4 signaling pathway in orthodontic tooth movement. BMC Oral Health. 2025; 25: 118. https://doi.org/10.1186/s12903-025-05491-8.

[47] Zhang Y, Kou Y, Yang P, Rong X, Tang R, Liu H, *et al*. ED-71 inhibited osteoclastogenesis by enhancing EphrinB2-EphB4 signaling between osteoclasts and osteoblasts in osteoporosis. Cellular Signalling. 2022; 96: 110376. http://doi.org/10.1016/j.cellsig.2022.

110376.

[48] Jiao Y, Wang X, Wang Q, Geng Q, Cao X, Zhang M, *et al*. Mechanisms by which kidney-tonifying Chinese herbs inhibit osteoclastogenesis: Emphasis on immune cells. Frontiers in Pharmacology. 2023; 14: 1077796. https://doi.org/10.3389/fphar.2023.1077796.

[49] Tang X, Huang Y, Fang X, Tong X, Yu Q, Zheng W, *et al*. *Cornus officinalis*: a potential herb for treatment of osteoporosis. Frontiers in Medicine. 2023; 10: 1289144. https://doi.org/10.3389/fmed.2023.1289144.

Editor's note: The Scientific Editor responsible for this paper was Bo Lei.

Received: 28th August 2025; **Accepted**: 18th December 2025; **Published**: 30th January 2026